

Nonlinearity Enhanced Adaptive Activation Function

David Yevick
Department of Physics
University of Waterloo
Waterloo, ON N2L 3G7
yevick@uwaterloo.ca

Abstract: A simply implemented activation function with even cubic nonlinearity is introduced that increases the accuracy of neural networks without substantial additional computational resources. This is partially enabled through an apparent tradeoff between convergence and accuracy. The activation function generalizes the standard RELU function by introducing additional degrees of freedom through optimizable parameters that enable the degree of nonlinearity to be adjusted. The associated accuracy enhancement is quantified in the context of the MNIST digit data set through a comparison with standard techniques.

Keywords: Activation functions, Machine Learning, Neural Networks, Pattern Recognition

1. Introduction:

While neural networks (NN) were first proposed in 1943 [1], initial implementations were restricted to networks with a small number of neurons and one or two layers[2], [3]. This limitation was eliminated through the backpropagation training algorithm[3], [4], [5] in conjunction with exponential improvements in computational performance. The resulting procedure generates a system model exclusively from experimental or simulated data and can accordingly be employed in a wide variety of scientific and engineering fields. In particular, a system, which typically can be characterized by a few coordinates and equations, is instead described by a large number of variables that interact nonlinearly. By optimizing a loss function, which may be further subject to physical constraints as in physics-informed machine

learning,[6] the parameters associated with the interactions are adjusted to approximate the data. The trained model then can predict the response of the system to unobserved input data.

Although such an approach possesses significant advantages in terms of generality and simplicity, it lacks the precision and efficiency afforded by the solution of deterministic equations. Similarly, the large dimensionality of the representation obscures the underlying physics and mathematics. For complex systems, however, especially in the presence of stochastic noise or measurement inaccuracy, procedures based on numerical optimization can be effectively optimal.[7], [8], [9], [10], [11]

Typical neural networks implement nonlinearity by inserting the data into the first of a series of layers of artificial neurons. Each neuron in a layer processes either the input data or the outputs of the previous layer by applying a nonlinear 'activation' function to the sum of a bias term and the product of each of its input values with a separate weighting factor. The collection of bias terms and weighting factors, which can be extensive in the case of deep neural networks with multiple layers, is then optimized.[12] The nonlinearity introduces curvature into the decision boundaries as can be visualized in PCA space,[13] significantly enhancing the discrimination capability of the network.

Numerous activation functions have been advanced since the threshold logic unit (linear threshold unit) was first introduced to model the response of biological neurons.[1] These activation functions can be classified as non-adaptive and adaptive. The former consists of a deterministic, generally monotonic, function. Although modest improvements can be realized with specialized profiles, the simplest, rectified linear unit (RELU), activation function often proves most efficient and therefore effective.[14], [15], [16] The RELU is linear for positive values of its argument and zero otherwise, corresponding to an ideal switch. Effectively, when a large network is optimized the characteristics of the activation function are often suppressed as the network compensates for these by adjusting the values of the free parameters.

The form of adaptive activation functions is parametrized by one or more variables that are optimized during training. While the predictive accuracy of the network is typically increased the improvement is often not sufficient to justify the additional coding and computational effort.[16], [17], [18], [19], [20], [21], [22], [23] A comprehensive study of activation functions is beyond the scope of this paper but can be found in e.g. [17], [24], [25], [26], [27] Generally, the optimal profile is problem dependent; however, as stated above, the practical improvement is typically not significant as it is offset by changes to the training parameters.

2. Activation Function: This paper introduces a, to our knowledge, novel activation function which, as the following section demonstrates, yields improved results despite being relatively simple to program and computationally efficient. The function structure is motivated by the standard **relu**, namely[14], [15]

$$f(x) = x\theta(x) \tag{1}$$

where $\theta(x)$ is the Heaviside step function. The nonlinearity associated with Eq.(1) originates from the slope discontinuity at $x = 0$. Although x is displayed as a scalar variable, in a neural network application for each layer l , it represents the vector argument $\mathbf{W}^{(l)}\vec{x}^{(l-1)} + \vec{b}^{(l)}$ of values generated from the outputs $\vec{x}^{(l-1)}$ of the previous neural network or input layer, where $\mathbf{W}^{(l)}$ and $\vec{b}^{(l)}$ are the associated weight matrix and bias vector, respectively. The function f is applied to each component of its argument.

An alternative to Eq. (1) is given by the **swish** activation function

$$f(x, \beta) = \frac{x}{1 + e^{-\beta x}} \tag{2}$$

where β can be either a constant or a trainable parameter.[16] Eq.(2) is similar in form to the **relu** but possesses a continuous derivative at the origin, which facilitates optimization.

To preserve the underlying features of the **relu** while improving its accuracy (a similar procedure can obviously be applied to the **swish** or any other activation function), a cubic term with layer-dependent coefficients is here added to the activation function according to

$$f^{(l)}(x, c_0^{(l)}, c_1^{(l)}) = \theta \left(c_0^{(l)}x + \gamma c_1^{(l)}x^2|x| \right) \quad (3)$$

with γ a user-specified constant. The absolute value in the cubic term introduces an even component into the function argument. The amplitudes of the two terms in the activation function are employed as additional parameters at each layer l of the neural network during training. While this adds only $2(N - 1)$ optimization parameters in the standard case of a N layer neural network with a **softmax** output layer, the computation time is somewhat affected by the cubic term. The global constant, γ , adjusts the strength of this term during the initial epochs, which as evident below affects both the probability of convergence and the accuracy of the resulting prediction.

3. Computational Results: The neural network employed in this paper is a straightforward extension of the easily modified computer code presented in p.63-66 of [28], as summarized in the appendix. The input data consists of the benchmark MNIST collection of 70,000 handwritten digits together with their associated labels discretized on a 28×28 point grid with 256 grayscale levels. These are divided into a training set of 60,000 digits and a test set of 10,000 digits and normalized to a maximum value of unity. The neural network, which consists of dense 512 and 50 neuron layers followed by a 10 neuron output layer with a **softmax** activation function, is trained with a **Nadam** optimizer and a batch size of 128 over 150 epochs. If the average digit accuracy remains at a value less than 0.5 (and in general close to 0.1) after 15 epochs, the calculation is prematurely terminated and the subsequent realization is started. This effectively eliminates the computational overhead of unconverged realizations.

To benchmark the adaptive activation function, Eq. (3), the test accuracy of the program described in the previous paragraph for a **relu** activation function in the 512 and 50 neuron layers is evaluated after every 2 epochs. Plotting these values as a function of epoch number for 60 separate calculations yields Figure 1(a). Figure 1(b), then displays a histogram of the accuracy of the final results for the range between 0.982 and 0.986. Since a small fraction of the MNIST digits are effectively impossible to classify, results in this range are highly precise. Further, 3 of the 180 calculations remained at accuracies less than $A_1 = 0.5$ after 15 epochs while an additional 5 calculations generated results, r , with $A_1 < r < A_2 = 0.982$. The first of these two sets of calculations were prematurely terminated and therefore did not substantively affect the computation time while the latter calculations are absent from the histogram of Figure 1. The corresponding results in Figure 2 for 60 calculations with the **swish** activation function, Eq.(2), demonstrate that the analyticity of the activation function induces a smooth, quasi-Gaussian distribution of the predicted values although the mean accuracy of the **swish** and **relu** calculations are similar. Additionally, only a single calculation was terminated with $r < A_1$ while for one calculation $A_1 < r < A_2$.

If the activation function of Eq.(3) is employed with $\gamma = 5$, the accuracy improves markedly as evident in Figure 3 for 150 calculations. At the same time, the number of non-converged results considerably increased to 63 with $r < A_1$ and 1 with $A_1 < r < A_2$. This suggests a tradeoff between predictive accuracy and convergence probability. Indeed, decreasing γ in Eq.(3) to 1 and 2.5 yields the results of Figure 4 (a) and (b), respectively for 60 realizations with corresponding $r < A_1$ and $A_1 < r < A_2$ values of (5,4) and (6, 2). As γ is lowered a larger percentage of calculations converge but the overall accuracy decreases towards the **relu** result. A possible explanation is that for larger γ the parameter space is more exhaustively sampled during the initial epochs, which enhances both the optimizer performance and the probabilities both of the system becoming trapped in local minima that inhibit convergence and those that yield the most accurate predictions.

The adaptive activation function of Eq. (3) for $\gamma = 1$ but without the absolute value sign in the cubic term generates the results of Figure 5 after 180 computations, where to achieve a reasonable probability of convergence the argument of Eq.(3) was replaced by $c_0^{(l)} + c_1^{(l)}x + \gamma c_2^{(l)}x^2|x|$. The resulting accuracy is somewhat less than that of Figure 1 and Figure 2 while the number of calculations with $r < T_1$ and $T_1 < r < T_2$ increases to 88 and 19, respectively. Evidently, the improvement afforded by Eq.(3) largely results from the presence of both odd and even terms in Eq.(3).

4. Conclusions and Future Directions: The numerical studies of this paper suggest several general conjectures regarding activation function properties. First, analytic activation functions appear to yield smoother distributions of neural network predictions. Secondly, a trade-off was observed by which more accurate solutions can be obtained by activation functions that generate a greater number of nonconverged results. Since these, however, can be rapidly identified and deleted, the computation time is largely unaffected. Finally, a simple yet highly accurate adaptive activation function was advanced with a, to our knowledge, novel structure. This activation function preserves the form of the **relu** function while adding an even cubic nonlinearity. Since the accuracy only increased for even parity, maximally effective adaptive functions could require separately adjustable even and odd components.

While the conclusions of the preceding paragraph appear speculative based on the few representative results presented, the activation function of Eq.(3) emerged from numerous trial calculations. Future work could presumably extend the analysis to other classes of activation functions, for example, by substituting a different even function for the cubic term or by replacing the theta function by more complex non-adaptive or adaptive activation functions. Given the extensive search space more optimal activation functions can presumably be identified which exhibit not only improved accuracy but also a smaller number of rejected calculations and a smoother final value distribution.

Acknowledgements: The Natural Sciences and Engineering Research Council of Canada (NSERC) is acknowledged for financial support. [grant number RGPIN-03907-2020]

Biography: David Yevick (Ph.D. 1979, F. OSA, IEEE, APS) is a professor of physics at the University of Waterloo having been previously at Queen’s University (Kingston), Penn State University ,Lund University and the Institute of Optical Research, Stockholm. He has published over 200 articles in optical communications, physics and computational methods.

Compliance with Ethical Standards: The research leading to these results received funding from the Natural Sciences and Engineering Research Council of Canada (NSERC) under grant agreement number RGPIN-03907-2020. The authors have no relevant financial or non-financial interests to disclose.

Appendix: The principal modifications of the code p.63-66 of [28] are as follows:

1)

```
def linear( x ):
    return x

class NaiveNonlinear:
    def __init__(self, input_size):
        output_size = 2
        b_shape = (output_size,)
        b_initial_value = ( tf.random.uniform(b_shape, minval = 0, maxval = 1e-2) )
        self.b = tf.Variable(b_initial_value)

    def __call__(self, inputs):
        g = 5
        return( tf.math.maximum( tf.add( self.b[0] * inputs, g * self.b[1] * tf.sign( inputs ) * inputs * inputs ), 0 ) )

    @property
    def weights(self):
        return [ self.b ]

    def set_weights(self, my_weights):
        [ self.b ] = my_weights

def model_body( train_images, train_labels ):
    model = NaiveSequential([
        NaiveDense(input_size=new_image_length, output_size = 512, activation = linear ),
```

```

NaiveNonlinear( intermediate_size1 ),
NaiveDense(input_size = 512, output_size = 50, activation = linear ),
NaiveNonlinear( intermediate_size2 ),
NaiveDense(input_size=intermediate_size2, output_size=10, activation = tf.nn.softmax )
])

```

2)

```

for loop in range( numberOfRepeats ):
    optimizer = tf.keras.optimizers.Nadam()
    model_body( train_images, train_labels )

```

References:

- [1] W. S. McCulloch and W. Pitts, "A logical calculus of the ideas immanent in nervous activity," *Bull Math Biophys*, vol. 5, no. 4, pp. 115–133, Dec. 1943, doi: 10.1007/BF02478259/METRICS.
- [2] C. M. BERNERS-LEE, "Cybernetics and Forecasting," *Nature 1968 219:5150*, vol. 219, no. 5150, pp. 202–203, Jul. 1968, doi: 10.1038/219202b0.
- [3] F. Rosenblatt, "The perceptron: A probabilistic model for information storage and organization in the brain," *Psychol Rev*, vol. 65, no. 6, pp. 386–408, Nov. 1958, doi: 10.1037/H0042519.
- [4] D. E. Rumelhart, G. E. Hinton, and R. J. Williams, "Learning representations by back-propagating errors," *Nature 1986 323:6088*, vol. 323, no. 6088, pp. 533–536, 1986, doi: 10.1038/323533a0.
- [5] Y. LeCun *et al.*, "Backpropagation Applied to Handwritten Zip Code Recognition," *Neural Comput*, vol. 1, no. 4, pp. 541–551, Dec. 1989, doi: 10.1162/NECO.1989.1.4.541.
- [6] G. E. Karniadakis, I. G. Kevrekidis, L. Lu, P. Perdikaris, S. Wang, and L. Yang, "Physics-informed machine learning," *Nature Reviews Physics 2021 3:6*, vol. 3, no. 6, pp. 422–440, May 2021, doi: 10.1038/s42254-021-00314-5.
- [7] S. O. Haykin, "Neural Networks: A Comprehensive Foundation." 1998.
- [8] M. Nielsen, "Neural Networks and Deep Learning." 2015.
- [9] R. Chellappa, S. Theodoridis, and A. Van Schaik, "Advances in Machine Learning and Deep Neural Networks," *Proceedings of the IEEE*, vol. 109, no. 5. 2021. doi: 10.1109/JPROC.2021.3072172.
- [10] G. E. Hinton and R. R. Salakhutdinov, "Reducing the dimensionality of data with neural networks," *Science (1979)*, vol. 313, no. 5786, pp. 504–507, Jul. 2006, doi: 10.1126/science.1127647.
- [11] P. Mehta *et al.*, *A high-bias, low-variance introduction to Machine Learning for physicists*, vol. 810. Elsevier B.V., 2019, pp. 1–124. doi: 10.1016/j.physrep.2019.03.001.

- [12] Y. Lecun, Y. Bengio, and G. Hinton, *Deep learning*, vol. 521, no. 7553. Nature Publishing Group, 2015, pp. 436–444. doi: 10.1038/nature14539.
- [13] D. Yevick and K. Hutchison, “Neural Network Characterization and Entropy Regulated Data Balancing through Principal Component Analysis,” Dec. 2023, Accessed: Mar. 16, 2024. [Online]. Available: <https://arxiv.org/abs/2312.01392v1>
- [14] V. M. Vargas, D. Guijo-Rubio, P. A. Gutiérrez, and C. Hervás-Martínez, “ReLU-Based Activations: Analysis and Experimental Study for Deep Learning,” *Lecture Notes in Computer Science (including subseries Lecture Notes in Artificial Intelligence and Lecture Notes in Bioinformatics)*, vol. 12882 LNAI, pp. 33–43, 2021, doi: 10.1007/978-3-030-85713-4_4.
- [15] O. Fuentes, J. Parra, E. Anthony, and V. Kreinovich, “Why Rectified Linear Neurons Are Efficient: A Possible Theoretical Explanation,” *Studies in Computational Intelligence*, vol. 835, pp. 603–613, 2020, doi: 10.1007/978-3-030-31041-7_34.
- [16] E. Alcaide, “E-swish: Adjusting Activations to Different Network Depths,” Jan. 2018, Accessed: Mar. 14, 2024. [Online]. Available: <http://arxiv.org/abs/1801.07145>
- [17] A. Apicella, F. Donnarumma, F. Isgrò, and R. Prevete, “A survey on modern trainable activation functions,” *Neural Networks*, vol. 138, pp. 14–32, Jun. 2021, doi: 10.1016/J.NEUNET.2021.01.026.
- [18] L. R. Sütfeld, F. Brieger, H. Finger, S. Füllhase, and G. Pipa, “Adaptive Blending Units: Trainable Activation Functions for Deep Neural Networks,” *Advances in Intelligent Systems and Computing*, vol. 1230 AISC, pp. 37–50, 2020, doi: 10.1007/978-3-030-52243-8_4/TABLES/3.
- [19] H. Gouk, B. Pfahringer, E. Frank, and M. J. Cree, “MaxGain: Regularisation of neural networks by constraining activation magnitudes,” *Lecture Notes in Computer Science (including subseries Lecture Notes in Artificial Intelligence and Lecture Notes in Bioinformatics)*, vol. 11051 LNAI, pp. 541–556, 2019, doi: 10.1007/978-3-030-10925-7_33.
- [20] L. R. Sütfeld, F. Brieger, H. Finger, S. Füllhase, and G. Pipa, “Adaptive Blending Units: Trainable Activation Functions for Deep Neural Networks,” *Advances in Intelligent Systems and Computing*, vol. 1230 AISC, pp. 37–50, 2020, doi: 10.1007/978-3-030-52243-8_4/TABLES/3.
- [21] M. Dushkoff and R. Ptucha, “Adaptive activation functions for deep networks,” *IS and T International Symposium on Electronic Imaging Science and Technology*, 2016, doi: 10.2352/ISSN.2470-1173.2016.19.COIMG-149.
- [22] F. Agostinelli, M. Hoffman, P. Sadowski, and P. Baldi, “Learning activation functions to improve deep neural networks,” *3rd International Conference on Learning Representations, ICLR 2015 - Workshop Track Proceedings*, 2015.
- [23] F. Manessi and A. Rozza, “Learning Combinations of Activation Functions,” *Proceedings - International Conference on Pattern Recognition*, vol. 2018-August, pp. 61–66, Nov. 2018, doi: 10.1109/ICPR.2018.8545362.

- [24] A. D. Jagtap and G. E. Karniadakis, "How important are activation functions in regression and classification? A survey, performance comparison, and future directions".
- [25] M. Gustineli, "A survey on recently proposed activation functions for Deep Learning," Apr. 2022, Accessed: Mar. 14, 2024. [Online]. Available: <https://arxiv.org/abs/2204.02921v2>
- [26] D. A. R. Sakthivadivel, "Formalising the Use of the Activation Function in Neural Inference," *Complex Systems*, vol. 31, no. 4, pp. 433–449, Feb. 2021, doi: 10.25088/ComplexSystems.31.4.433.
- [27] M. Goyal, R. Goyal, P. Venkatappa Reddy, and B. Lall, "Activation functions," *Studies in Computational Intelligence*, vol. 865, pp. 1–30, 2020, doi: 10.1007/978-3-030-31760-7_1.
- [28] F. Chollet, *Deep {Learning} with {Python}, {Second} {Edition}*, 2nd edition. Shelter Island: Manning, 2021.

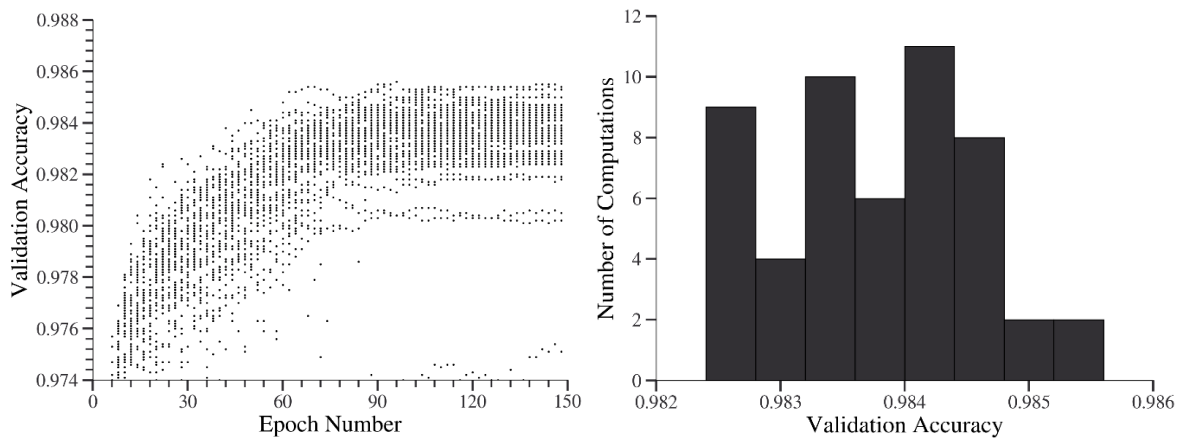


Figure 1: The test accuracy during and after 60 separate calculations for a 512/50/10 dense neural network with a **relu** activation function. In the left figure, Figure 1(a), the test accuracy is evaluated in each calculation after every 2 epochs while the right figure, Figure 1(b), displays a histogram of the final accuracy of each computation.

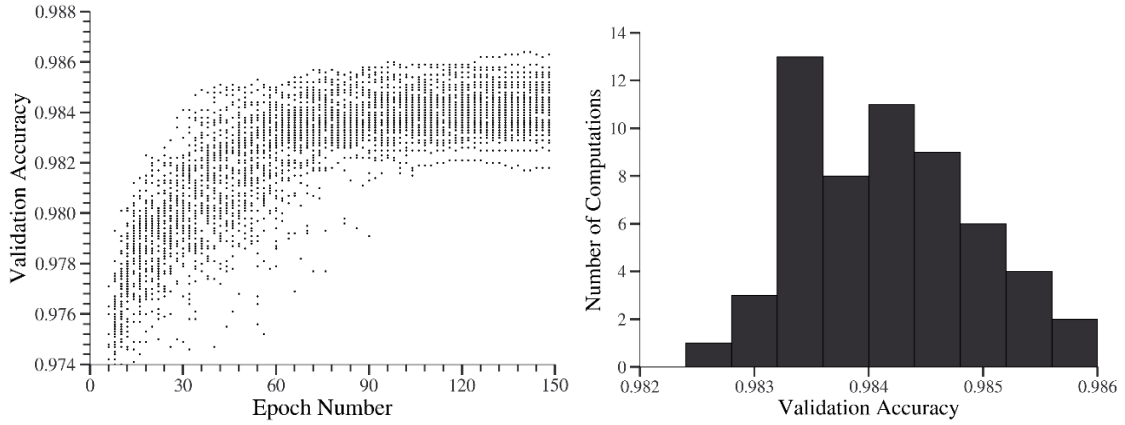


Figure 2: As in Figure 1 but for a *swish* activation function.

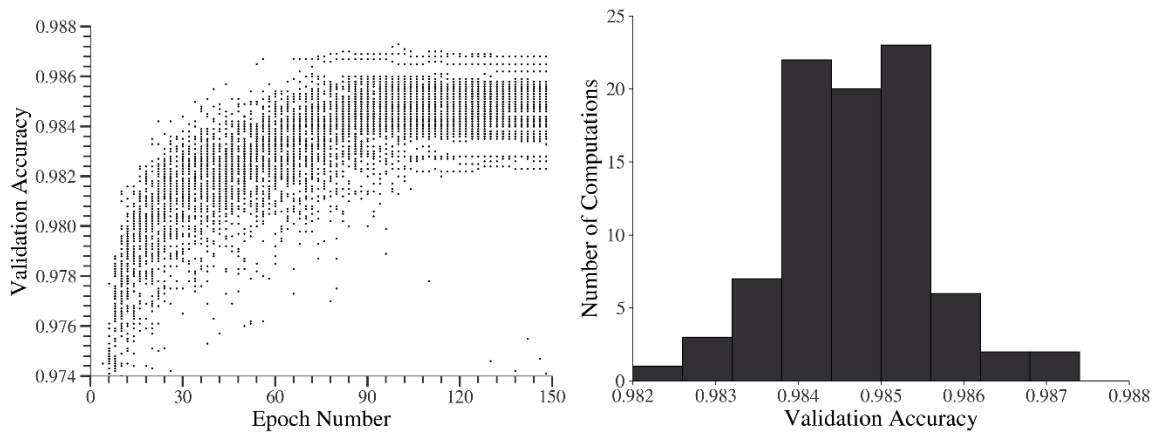


Figure 3: As in Figure 1 but for the activation function introduced in this paper with $\gamma = 5$ and 150 realizations. Note the expanded x-axis scale in (b).

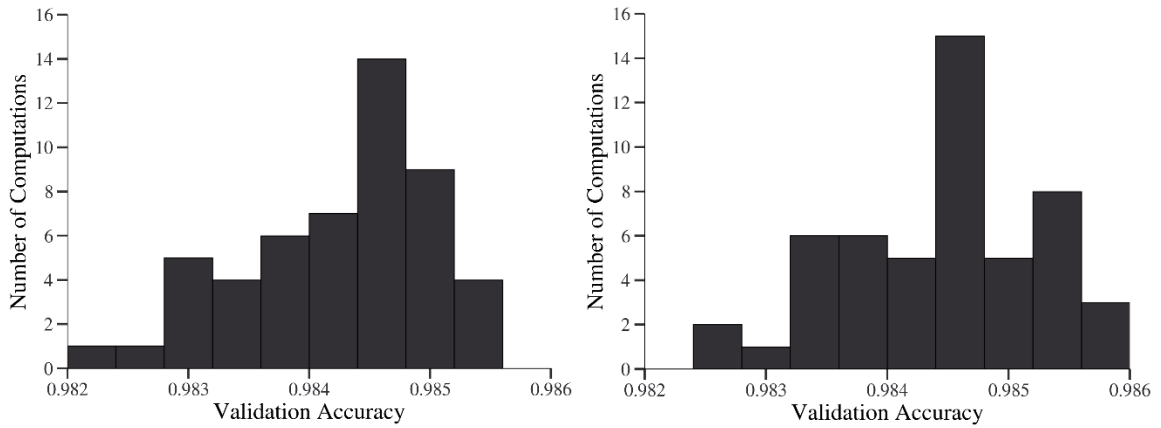


Figure 4: The histogram of Figure 3 but for $\gamma = 1$ (left plot) and $\gamma = 2.5$ (right plot) and 60 realizations.

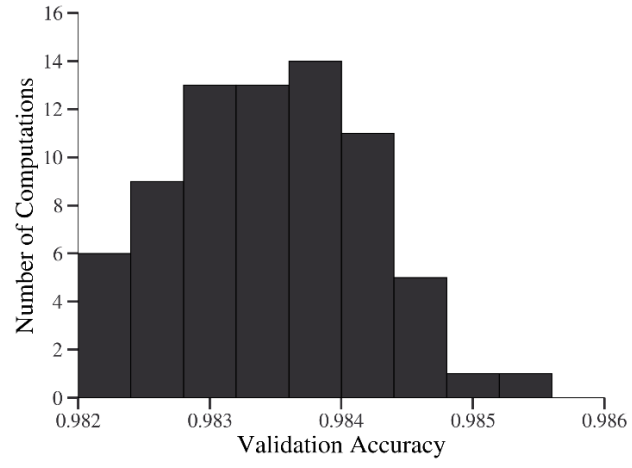


Figure 5: The histogram of Figure 3 with $\gamma = 1$ and without absolute value sign in the cubic term in the activation function for 180 realizations.